A EUROPEAN JOURNAL OF CHEMICAL BIOLOGY

CHEMBIOCHEM

SYNTHETIC BIOLOGY & BIO-NANOTECHNOLOGY

Accepted Article

Title: Compartments for Synthetic Cells: Osmotically Assisted Separation of Oil from Double Emulsions in Microfluidic Chip

Authors: Dorothee Krafft, Sebastian Lopez-Castellanos, Rumiana Dimova, Ivan Ivanov, and Kai Sundmacher

To be cited as: *ChemBioChem* 10.1002/cbic.201900152

Link to VoR: http://dx.doi.org/10.1002/cbic.201900152

A Journal of

ChemPubSoc Europe

WILEY-VCH

www.chembiochem.org

10.1002/cbic.201900152

WILEY-VCH

COMMUNICATION

Compartments for Synthetic Cells: Osmotically Assisted Separation of Oil from Double Emulsions in Microfluidic Chip

Dorothee Krafft,[a]† Sebastián López Castellanos,[a]† Rumiana Dimova,[b] Ivan Ivanov,[a]* and Kai Sundmacher[a,c]

Abstract: Liposomes are used in synthetic biology as cell-like compartments and their microfluidic production via double emulsions allows for efficient encapsulation of various components. However, the residual oil in the membrane remains a critical bottleneck for creating pristine phospholipid bilayers. We discovered that osmotically driven shrinking leads to detachment of the oil drop. We realized the separation inside a microfluidic chip in order to automate the procedure, which allowed for controlled continuous production of monodisperse liposomes.

Giant unilamellar vesicles (GUVs) are widely used as model membranes to study the biophysical properties of phospholipid bilayers.[1-3] In parallel, they attract increasing attention as cell-like compartments in bottom-up synthetic biology, where the long-term goal is to build a minimal cell from scratch.[4-8] When selecting GUV production method for synthetic biology, the ability to encapsulate various components is essential.[2] Conventional methods for the production of liposomes comprise gentle hydration[9-10], swelling on polymer cushions[11-12] and electro-formation.[13-14] These methods are not always optimal due to the low GUV yield in physiological buffer, the poor encapsulation efficiency[2, 15-16] and in some cases the harsh conditions that delicate biomolecules and smaller vesicles are exposed to during the preparation.[17] This issue has been addressed by the phase transfer method, which is based on pre-formed w/o emulsion droplets, crossing a second o/w interface.[18] In the last years several other, conceptually similar, methods have been developed, aiming to provide higher productivity and better control, namely microfluidic jetting[19], cDICE[20], microfluidic formation of droplet-stabilized vesicles[21] and microfluidic production of w/o/w double emulsions.[22] The latter approach appears to be the least experimentally demanding and multiple setups for double emulsion production have been proposed. Microfluidic chips made out of glass[17, 22] or PDMS[23-26] and organic phases such as octanol[24], chloroform/hexane[17] and oleic acid[27] have been used to produce stable double emulsions, which have found attractive applications for synthetic biology such as the encapsulation of smaller vesicles, proteins and DNA.[17, 24, 28] Another advantage of the double emulsion procedure is the virtual absence of losses with respect to the encapsulated solutions and therefore it is suitable for valuable substrates, available in low quantities.

In addition to efficient encapsulation, mimicking nature requires a pristine bilayer, which would not compromise membrane-related phenomena, such as the folding of reconstituted membrane proteins. However, the presence of residual oil is an inherent vice of GUVs prepared from double emulsions, which necessitates removal of the organic phase. So far, a few approaches for solvent removal have been shown: evaporation[29], spontaneous splitting off[17, 24] and squeezing.[30] Here, we present another, simple method to separate oil from double emulsions and to generate GUVs. We show that oleic acid droplets exhibit complete dewetting from the deflating vesicles when exposed to osmotic gradient. The latter shrinking effect has been very recently used as a tool for manipulation of concentration and size [31] but to the best of our knowledge, its use to detach the oil droplet has not been demonstrated. We also integrate the osmotic dewetting into a microfluidic chip to observe the process and to achieve a certain degree of modularity and automation.

We used a microfluidic chip design with two junctions for the initial formation of double emulsion (Fig. 1 and Movie S1), similar to the commonly used.[25-27] Briefly, w/o emulsions were formed at the first junction, followed by crossing a second junction with the aqueous outer fluid (OF), which resulted in highly monodisperse w/o/w emulsions at 40–50 Hz. The walls of the chip after the second junction were coated with 1% PVA for hydrophilization to ensure proper formation of the double emulsion. The size of the w/o/w emulsions strongly depends on the size of the aqueous droplets formed at the first junction, which can be in turn controlled to a certain extent by the different flow rates and the chip design (*e.g.* channel width).

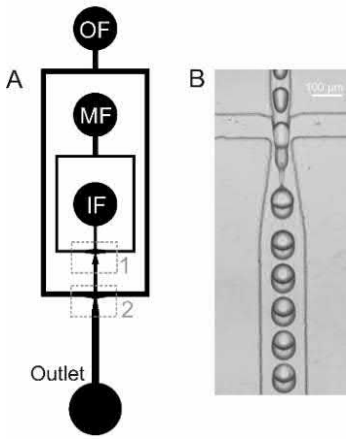

Figure 1. (A) Microfluidic design of the PDMS-chip for double emulsion formation. OF: outer fluid, MF: middle fluid, IF: inner fluid. 1st and 2nd junction marked as 1 and 2; (B) Microscopic image of the 2nd junction.

[a] D. Krafft, S. López Castellanos, I. Ivanov, K. Sundmacher
Process Systems Engineering, Max Planck Institute for Dynamics of Complex Technical Systems, Sandtorstrasse 1, 39106 Magdeburg, Germany.
E-Mail: ivanov@mpi-magdeburg.mpg.de
[b] R. Dimova
Max Planck Institute of Colloids and Interfaces, Science Park Golm, 14424 Potsdam, Germany.
[c] K. Sundmacher
Otto-von-Guericke University Magdeburg, Universitätsplatz 2, 39106 Magdeburg, Germany.

† These authors contributed equally.

Supporting information for this article is given via a link at the end of the document.

In the present case, the size of the w/o/w emulsions ranged from 40 to 70 µm. There was no exchange between inner fluid (IF) and OF and small volumes (less than 500 µl) of IF were used for the preparation. Using the setup described by Petit[27] as a starting point, we reduced the number of components to create stable double emulsions with minimal composition: 200 mM sucrose as IF, 10 mg ml^{-1} L-α-phosphatidylcholine (soy PC) in oleic acid as MF, and 200 mM sucrose + 1wt% Pluronic F108 as OF. The surfactant Pluronic F108 was added to ensure stability of the double emulsion during its formation. The typical flow rates were 40 µl h^{-1} for IF and MF, and 400 µl h^{-1} for OF.

The utilization of different oil phases for the production of w/o/w emulsions has led to different methods for subsequent oil removal. Extraction of oleic acid with ethanol[26-27] as reported in the literature was not successful in the present case because it did not result in any apparent decrease of oleic acid in the membrane (Fig. S1). In addition, high ethanol concentrations[27] might not be compatible with certain encapsulated components. However, we were able to observe partial and sometimes full dewetting when observing the double emulsions under microscope on a glass slide (Fig. S2). We attributed the observed phenomenon to the interplay of interfacial tensions and the osmotic imbalance between IF and OF resulting from evaporation of the sample. To test this hypothesis, we first eliminated the evaporation by placing a cover slide, which resulted in partial dewetting, but no full dewetting at equal osmolarity (Fig. 2). We then gradually changed the osmotic gradient between IF and OF by sucrose and sodium chloride and eventually, reducing the IF solute concentration to ¼ compared to the OF resulted in full dewetting (Fig. S3&4).

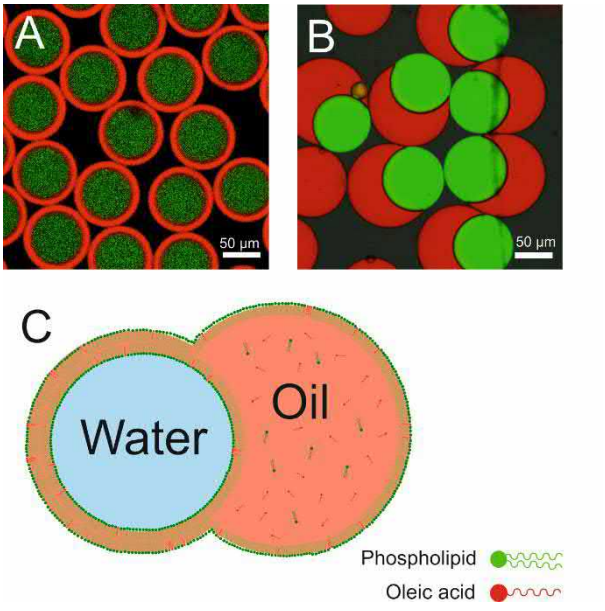

Figure 2. (A) Confocal image of the double emulsion immediately after formation; (B) Confocal image of the partially dewetted vesicle. Nile red (red), dissolved in the MF was used to stain the oil and the lipid membrane and fluorescein dextran (green) was encapsulated in the aqueous IF. (C) Schematic representation of the partially dewetted vesicle. Note that the orange color of the oil pocket corresponds to oleic acid and that color designation of the phospholipids does not correspond to A and B.

In presence of said osmotic gradient, comparison of the interfacial tension between MF and IF ($\gamma_{MF\text{-}IF}$ = 11.05 mN m^{-1}) with the value between MF and OF ($\gamma_{MF\text{-}OF}$ = 0.04 mN m^{-1}) suggests that the interfacial tension between IF and OF ($\gamma_{IF\text{-}OF}$) is in the range of $\gamma_{MF\text{-}IF} \pm \gamma_{MF\text{-}OF}$ (11.01–11.09 mN m^{-1}). Values above this range would prevent partial dewetting and lower values would result in spontaneous full dewetting as reported by Deng[32]. As the osmotic gradient deflates the vesicle to match the osmolarity of the IF and OF, which might be facilitated by the presence of surfactants in the membrane, the cup-shaped bilayer (Fig. 2) enwraps the reduced aqueous volume. We believe that the force balance at the interfacial three-phase contact line is not significantly changed by the osmotic gradient itself as the interfaces composition is not expected to change significantly by the changes of the solute concentration in the aqueous phases. Simple geometric considerations allow to calculate the necessary volume reduction to obtain a free vesicle. Assuming a vesicle, whose surface is 50% dewetted, its volume should be reduced by a factor of $2*\sqrt{2}$ in order to be enclosed by the existing (dewetted) bilayer (see Supporting Information).

Even though in the majority of the cases more than 50% of the surface area was dewetted, we opted for a four-fold volume reduction (proportional to the osmolarity) to ensure that the dewetted surface was sufficient to enclose the reduced volume. We ascribed the final detachment of the oil pocket from the vesicle to the gentle agitation during the manipulation, which aided the scission of the neck connecting the GUV and the droplet at the transient conditions (Fig. S2). Otherwise the nearly fully dewetted vesicle (with reduced volume now) would undergo partial wetting again until reaching the initial energetically favorable equilibrium.

In order to test whether the dewetted membrane was a phospholipid bilayer without residual oil, we used Nile red and a fluorescent lipid (PE-CF, dioleoylphosphoethanolamine-N-carboxyfluorescein), dissolved in the MF along with the soy PC. Nile red is a lipophilic dye, which is used to visualize intracellular lipids[33] but is also known to incorporate into phospholipid membranes.[34] In the present case (and for the specific imaging conditions), Nile red was almost exclusively located in the oleic acid pocket and barely visible in the dewetted membrane, while PE-CF was distributed between the membrane and the oil pocket (Fig. 3, fluorescence intensity profiles of partially dewetted vesicles in Fig. S5).

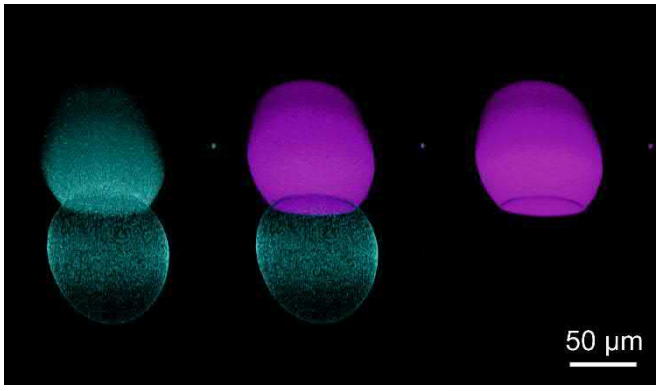

Figure 3. Confocal z-stack images of the partially dewetted vesicle and the attached oil pocket. Nile red (magenta) and PE-CF (cyan).

This implies preferential partitioning of Nile red in the oleic acid phase. We speculate that the apparent absence of Nile red in the dewetted part suggests a negligible amount of residual oil. However, this cannot be unequivocally confirmed in the limited scope of this study, especially provided that oleic acid is known to incorporate into the phospholipid membrane, which was in turn used to drive growth in protocell experiments.[35-36] From a

conceptual and practical point of view, the presence of minute amounts of oleic acid should still result in a realistic mimic of natural membranes since oleic acid is a natural precursor for the phospholipid synthesis. In addition, there are indications that a ligase, involved in the β-oxidation (FadD) converts oleic acid to the CoA-ester after its partitioning in the membrane, even though the protein is cytosolic.[37], which was also discussed in the context of membrane growth.

The potential presence of oleic acid would influence the properties of the bilayer depending on its concentration and might have adverse influence on the stability and permeability – membranes containing oleic acid are known to be less stable[38-39] – but this effect is yet to be determined with respect to the specific application. Increased permeability for certain small molecules may actually speed up osmotic deflation and also facilitate the transport of substrates for metabolic reactions, encapsulated in GUVs. The oleic acid pocket of partially dewetted vesicles has also found a useful application, enabling the reversible shrinking of liposomes by acting as a membrane reservoir.[31]

The osmotic gradient, sufficient for full dewetting, was determined based on observations of 10–15 µl w/o/w emulsion suspension, applied on a microscope slide. This setup was suitable for initial screening but it only allowed for collection of a few µl of the detached vesicle suspension for further experiments. Therefore, to increase the processing productivity, we automated the vesicle dewetting in a simple microfluidic chip and observed the time course of the process (approx. 80 s) through microscopy (Fig. 4, Fig. S6 and Movie S2). The height of the separation chip was kept at 70 µm (nearly matching the emulsion size) in order to ensure slight dragging of the oil pockets upon contact with the upper wall and thus to aid the splitting, in addition to the beneficial influence of the hydrodynamic flow. To separate the vesicles from the detached oil pockets, it sufficed to take advantage of the density difference between oleic acid and the aqueous solution (oil droplets floated at the top of the collection tube).

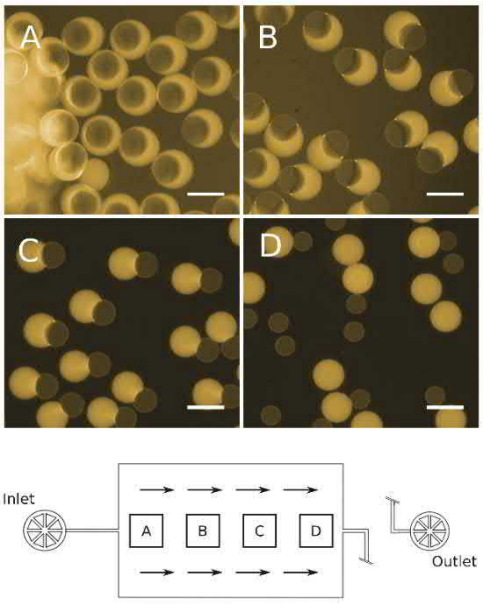

Figure 4. (A-D) Fluorescent images along the length of the chip, showing the dewetting and the detachment of the oil pockets. Liss-Rho-PE, dioleoylphosphoethanolamine-N-lissamine rhodamine B sulfonyl (yellow), dissolved in the MF was used to stain the oil and the lipid membrane. Relative imaging positions are shown at the bottom. Scale bar 100 µm.

We note that the dewetting chip is not essential for the splitting process. The detachment could theoretically be done by simply exposing the double emulsions to an osmotic gradient in an Eppendorf tube and mild centrifugation. However, using the dewetting chip has the advantage that the process can be observed under microscope, which in turn enables the optimization of detachment conditions (*e.g.* flow rate). Furthermore, the dewetting chip can be connected directly to the preceding double emulsion chip, which, after appropriate matching of flow rates and scaling of size, would allow for a high throughput generation of dewetted vesicles.

The resulting GUVs (Fig. 5), stained with Liss-Rho-PE in the membrane and fluorescein dextran in the IF, show no residual oil or lipid pockets in the membrane and are highly monodisperse, in contrast to electroformation (Fig. S7). The distribution of fluorescein dextran is also uniform across the individual liposomes (fluorescence intensity shows a standard deviation of 7.8% and interquartile range of 6% with respect to the mean value, compared to 7.1% and 11.3%, respectively, in the case of electroformation).

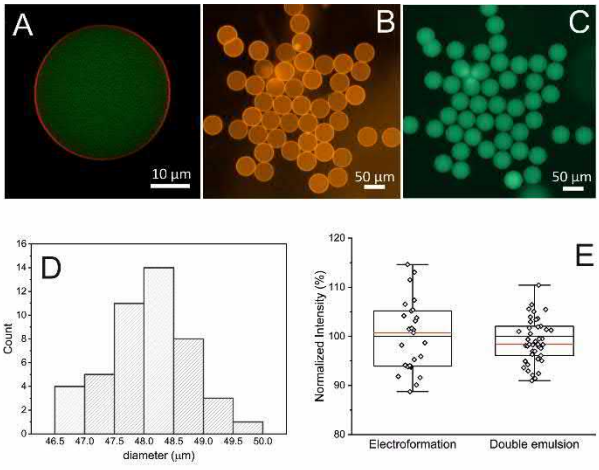

Figure 5. (A) Confocal image of a single vesicle; (B,C) Fluorescent images of dewetted vesicles after processing in a microfluidic chip for detachment. Liss-Rho-PE (orange), dissolved in the MF was used to stain the lipid membrane, fluorescein dextran (green) was encapsulated in the aqueous IF; (D) Size distribution of the dewetted vesicles; (E) Fluorescein dextran intensities of vesicles produced via electroformation and double emulsion. Note that the values have been normalized to the mean to ease the comparison.

Regarding the desired native state of the membrane, we should mention an issue, which has not been discussed before but is inherent to the double emulsion method. The production of stable double emulsions requires the use of a surfactant (Pluronic F108 in the present case), which may also affect the membrane properties. The influence of poloxamers has been studied in different contexts and depends on their structure – generally hydrophobic copolymers act as permeants, while hydrophilic ones seal the membrane.[40] Some reported effects are mechanical stabilization[41] and protection of vesicles against peroxidation[42], while in other cases Pluronic F108 increased the permeability for small molecules[43] and was used for lentiviral transduction.[44] Increased permeability should not necessarily be considered as a canonical drawback for synthetic biology applications because this could provide a feasible mechanism for membrane transport in bioreactor-type systems (which is otherwise attained by pore-forming agents[5]), provided that the vesicles retain their overall structural integrity and segregate the encapsulated machinery, *i.e.* enzymes. In addition, the conventional methods for

reconstitution of membrane proteins also involve the use of surfactants, which perturb the bilayer structure and are subsequently removed.[45] In this context, the adsorption and insertion of poloxamers exhibit different timescales[46-47], while the desorption is as fast as the adsorption[48], which provides a feasible mechanism for surfactant displacement by washing. Yet, the influence of residual surfactant and oil has to be determined in each specific case, depending on the intended application.

In conclusion, we have shown a new and simple method for oil removal to produce GUVs from w/o/w double emulsions. The exposure of double emulsions to osmotic gradients results in shrinking of the aqueous compartment, which causes the detachment of the oil phase. Thus, we circumvent the suboptimal interfacial tensions balance. As a result, liposomes without visible oil and lipid reservoirs are formed. The high encapsulation efficiency, the experimental flexibility and the mild conditions during the vesicle production potentially allow the encapsulation of complex and delicate compounds such as proteins, DNA and smaller vesicles, which could aid the construction of cell-like compartments in bottom-up synthetic biology.

Experimental Section

Experimental Details are given in the Supporting Information.

Acknowledgements

This work is part of the MaxSynBio consortium which is jointly funded by the Federal Ministry of Education and Research in Germany and the Max Planck Society. We thank Julien Petit for providing the initial double emulsion microfluidic design, Laura Turco for the preparation of silicon wafers and Martin Feneberg for additional support.

Conflict of Interest

The authors declare no conflict of interest.

Keywords: giant unilamellar vesicles • microfluidics • oleic acid • double emulsion • encapsulation

[1] R. Dimova, K. A. Riske, S. Aranda, N. Bezlyepkina, R. L. Knorr, R. Lipowsky, *Soft Matter* **2007**, *3*, 817-827.
[2] P. Walde, K. Cosentino, H. Engel, P. Stano, *ChemBioChem* **2010**, *11*, 848-865.
[3] R. Dimova, *Annu. Rev. Biophys*. **2019**, *48*, 93-119.
[4] D. Merkle, N. Kahya, P. Schwille, *ChemBioChem* **2008**, *9*, 2673-2681.
[5] V. Noireaux, A. Libchaber, *Proc. Natl. Acad. Sci. USA* **2004**, *101*, 17669-17674.
[6] P. Schwille, in *The Minimal Cell*, Springer, **2011**, pp. 231-253.
[7] H. Terasawa, K. Nishimura, H. Suzuki, T. Matsuura, T. Yomo, *Proc. Natl. Acad. Sci. USA* **2012**, *109*, 5942-5947.
[8] P. Walde, *Bioessays* **2010**, 32, 296-303.
[9] L. Bagatolli, T. Parasassi, E. Gratton, *Chem. Phys. Lipids* **2000**, *105*, 135-147.
[10] K. Tsumoto, H. Matsuo, M. Tomita, T. Yoshimura, *Colloids Surf., B* **2009**, *68*, 98-105.
[11] K. S. Horger, D. J. Estes, R. Capone, M. Mayer, *J. Am. Chem. Soc.* **2009**, *131*, 1810-1819.
[12] A. Weinberger, F. C. Tsai, G. H. Koenderink, T. F. Schmidt, R. Itri, W. Meier, T. Schmatko, A. Schroder, C. Marques, *Biophys. J.* **2013**, *105*, 154-164.
[13] M. I. Angelova, D. S. Dimitrov, *Faraday Discuss. Chem. Soc.* **1986**, *81*, 303-311.
[14] L.-R. Montes, A. Alonso, F. M. Goni, L. A. Bagatolli, *Biophys. J.* **2007**, *93*, 3548-3554.
[15] H. Stein, S. Spindler, N. Bonakdar, C. Wang, V. Sandoghdar, *Front. Physiol.* **2017**, *8*, 63.
[16] B. Sun, D. T. Chiu, *Anal. Chem.* **2005**, *77*, 2770-2776.
[17] N.-N. Deng, M. Yelleswarapu, L. Zheng, W. T. Huck, *J. Am. Chem. Soc.* **2016**, *139*, 587-590.
[18] S. Pautot, B. J. Frisken, D. A. Weitz, *Langmuir* **2003**, *19*, 2870-2879.
[19] J. C. Stachowiak, D. L. Richmond, T. H. Li, A. P. Liu, S. H. Parekh, D. A. Fletcher, *Proc. Natl. Acad. Sci. USA* **2008**, *105*, 4697-4702.
[20] M. Abkarian, E. Loiseau, G. Massiera, *Soft Matter* **2011**, *7*, 4610-4614.
[21] B. Haller, K. Göpfrich, M. Schröter, J.-W. Janiesch, I. Platzman, J. P. Spatz, *Lab Chip* **2018**, *18*, 2665-2674.
[22] L. Arriaga, E. Amstad, D. Weitz, *Lab Chip* **2015**, *15*, 3335-3340.
[23] W.-A. C. Bauer, M. Fischlechner, C. Abell, W. T. Huck, *Lab Chip* **2010**, *10*, 1814-1819.
[24] S. Deshpande, Y. Caspi, A. E. Meijering, C. Dekker, *Nat. Commun.* **2016**, *7*, 10447.
[25] K. Karamdad, R. Law, J. Seddon, N. Brooks, O. Ces, *Lab Chip* **2015**, *15*, 557-562.
[26] S.-Y. Teh, R. Khnouf, H. Fan, A. P. Lee, *Biomicrofluidics* **2011**, *5*, 044113.
[27] J. Petit, I. Polenz, J.-C. Baret, S. Herminghaus, O. Bäumchen, *Eur. Phys. J. E* **2016**, *39*, 59.
[28] N. N. Deng, W. T. Huck, *Angew. Chem.* **2017**, *129*, 9868-9872.
[29] H. C. Shum, D. Lee, I. Yoon, T. Kodger, D. A. Weitz, *Langmuir* **2008**, *24*, 7651-7653.
[30] A. Vian, V. Favrod, E. Amstad, *Microfluid. Nanofluid.* **2016**, *20*, 159.
[31] N.-N. Deng, M. Vibhute, L. Zheng, H. Zhao, M. Yelleswarapu, W. T. Huck, *J. Am. Chem. Soc.* **2018**, *140*, 7399-7402.
[32] N.-N. Deng, M. Yelleswarapu, W. T. Huck, *J. Am. Chem. Soc.* **2016**, *138*, 7584-7591.
[33] I. Sitepu, L. Ignatia, A. Franz, D. Wong, S. Faulina, M. Tsui, A. Kanti, K. Boundy-Mills, *J. Microbiol. Methods* **2012**, *91*, 321-328.
[34] O. A. Kucherak, S. Oncul, Z. Darwich, D. A. Yushchenko, Y. Arntz, P. Didier, Y. Mély, A. S. Klymchenko, *J. Am. Chem. Soc.* **2010**, *132*, 4907-4916.
[35] N. Berclaz, M. Müller, P. Walde, P. L. Luisi, *J. Phys. Chem. B* **2001**, *105*, 1056-1064.
[36] M. M. Hanczyc, S. M. Fujikawa, J. W. Szostak, *Science* **2003**, *302*, 618-622.
[37] M. Exterkate, A. Caforio, M. C. Stuart, A. J. Driessen, *ACS Synth. Biol.* **2017**, *7*, 153-165.
[38] I. A. Chen, R. W. Roberts, J. W. Szostak, *Science* **2004**, *305*, 1474-1476.
[39] P. Peterlin, V. Arrigler, K. Kogej, S. Svetina, P. Walde, *Chem. Phys. Lipids* **2009**, *159*, 67-76.
[40] C.-Y. Cheng, J.-Y. Wang, R. Kausik, K. Y. C. Lee, S. Han, *Biomacromolecules* **2012**, *13*, 2624-2633.
[41] K. Kostarelos, T. F. Tadros, P. Luckham, *Langmuir* **1999**, *15*, 369-376.
[42] J.-Y. Wang, J. Marks, K. Y. C. Lee, *Biomacromolecules* **2012**, *13*, 2616-2623.
[43] M. Jamshaid, S. Farr, P. Kearney, I. Kellaway, *Int. J. Pharm.* **1988**, *48*, 125-131.
[44] I. Höfig, M. J. Atkinson, S. Mall, A. M. Krackhardt, C. Thirion, N. Anastasov, *J. Gene Med.* **2012**, *14*, 549-560.
[45] A. M. Seddon, P. Curnow, P. J. Booth, *Biochim. Biophys. Acta, Biomembr.* **2004**, *1666*, 105-117.
[46] J. Y. Wang, J. M. Chin, J. D. Marks, K. Y. C. Lee, *Langmuir* **2010**, *26*, 12953-12961.
[47] G. Wu, K. Y. C. Lee, *J. Phys. Chem. B* **2009**, *113*, 15522-15531.
[48] M. Johnsson, N. Bergstrand, K. Edwards, J. J. Stålgren, *Langmuir* **2001**, *17*, 3902-3911.

Supporting Information

Experimental section

1.1 Materials

L-α-phosphatidylcholine (soy) (Soy PC, Avanti Polar Lipids), oleic acid 97% (AcrosOrganics), sodium chloride (Carl Roth), sucrose (Sigma Aldrich), Pluronic F108 (Sigma Aldrich), poly(vinyl alcohol) (PVA, MW 9000–10000, 80% hydrolized , Sigma Aldrich), fluorescein isothiocyanate-dextran (average MW 20000, Sigma Aldrich), 1,2-dioleoyl-sn-glycero-3-phosphoethanolamine-N-(lissamine rhodamine B sulfonyl) (ammonium salt) (Liss-Rho-PE) (Avanti Polar Lipids), 1,2-dioleoyl-sn-glycero-3-phosphoethanolamine-N-(carboxyfluorescein) (ammonium salt) (PE-CF) (Avanti Polar Lipids), Nile Red (Sigma Aldrich).

1.2 Fabrication and coating of the PDMS chip for double emulsion production

The design and the preparation of the double emulsion chip were described previously [1]. The silicon masks for both designs were prepared with soft lithography[2, 3]. Silicon wafers (4 inches, Si-Mat) were spin coated with SU-8 3050 (MicroChem, USA) for 2250 rpm for 30 s to achieve a height of around 70 µm. The photomask was a film mask (Micro Litho, UK) and alignment and UV exposure was done with a UV-KUB 3 (KLOE, France). After UV exposure for 5 s, the wafer was baked on a hot plate and the unexposed photoresist was dissolved by a developer. Afterwards the wafer was cleaned with isopropanol and a 10:1 mixture of poly(dimethyl siloxane) base and crosslinker (PDMS, Sylgard 184, Dow Corning, USA) was poured on the wafer. The PDMS was degassed in vacuum and baked at 80 °C for at least 4 h. Then the cured PDMS was cut with a scalpel and holes for the inlets and outlets were made with a biopsy puncher. A 24×50 mm microscopy glass coverslip was bonded to the PDMS chip after 1 min air plasma treatment (Plasma Cleaner PDC 32-G-2, Harrick Plasma, USA). The outer fluid channel of the double emulsion chips was coated with 1 wt% PVA for 1 min after the plasma treatment and afterwards incubated at 120 °C for at least 20 min. To ensure that only the channel for the OF was coated, the other two inlets were left open to allow air flow through the other channels. To prevent vesicles from bursting, the dewetting chip was incubated with 1% BSA for 30 min directly before use.

1.3 Fluid compositions

The inner and outer solutions were filtered (0.2 µm) to prevent potential blocking of the microfluidic channels. The inner fluid (IF) was composed of varying concentrations of sucrose and NaCl and in some cases fluorescein isothiocyanate-dextran was added at a final concentration of 0.1 mg ml^{-1}. The middle fluid (MF) was prepared by drying the necessary amount of soy PC lipids in a glass vial under nitrogen for at least 30 min. Afterwards oleic acid was added to a final lipid concentration of 10 mg ml^{-1}. To ensure proper dispersion of the lipids in the oil, the mixture was incubated for at least 1 h and vortexed frequently. Depending on the application, either Nile Red, Liss-Rho-PE or PE-CF were added as fluorescent dyes for the lipid phase. Nile Red was used at a final concentration of 1.6 µg ml^{-1} and Liss-Rho-PE as well as PE-CF

at a final concentration of 0.01 mg ml^{-1}. The outer fluid was composed of varying concentrations of sucrose and NaCl with an addition of 1 wt% of Pluronic F108 to stabilize the formation of the double emulsion.

1.4 Microfluidic double emulsion generation

For the production of double emulsion, syringes filled with IF, MF and OF were placed into neMESYS syringe pumps (Cetoni, Germany). The syringes were connected to the respective chip inlets with polytetrafluoroethylene (PTFE) tubing (0.56 mm inner diameter, 1.07 mm outer diameter, Adtech Polymer Engineering) and the outlet was connected to an Eppendorf tube. Double emulsions were formed at a rate of approximately 40–50 Hz and the formation was monitored under a microscope using a high-speed camera (Phantom, Phantom Vision, USA). Stable double emulsions could be achieved at flow rates around 40 µl h^{-1} (IF), 40 µl h^{-1} (MF) and 400 µl h^{-1} (OF). Variation of the flow rates allowed to some extent for manipulation of the size and MF/IF ratio of the double emulsions.

1.5 Microfluidic dewetting

Dewetting was achieved by pumping the double emulsion suspension through a dewetting chip at flow rates between 100 and 300 µl h^{-1}. However, when connecting the dewetting chip to the double emulsion chip, rates up to 500 µl h^{-1} were possible. Dewetting was monitored by fluorescent microscopy and the flow rate was adjusted if necessary. The osmotic gradient between IF and OF was 1:4.

1.6 Interfacial tensions

According to the literature [4], it is possible to ascribe the dewetting behaviour of a double emulsion to the interplay of the three interfacial tensions in the system, $\gamma_{IF\text{-}MF}$ (between IF and MF), $\gamma_{MF\text{-}OF}$ (between MF and OF) and $\gamma_{IF\text{-}OF}$ (between IF and OF) and the corresponding spreading coefficients of each of the three phases involved.

For partial dewetting to take place, the spreading coefficient of oil S_O needs to be negative, i.e.:

$$S_O = \gamma_{IF\text{-}OF} - (\gamma_{IF\text{-}MF} + \gamma_{MF\text{-}OF}) < 0$$

or: $\boldsymbol{\gamma_{IF\text{-}OF} < \gamma_{IF\text{-}MF} + \gamma_{MF\text{-}OF}}$

Further, the spreading coefficient S_{IF} of the IF also needs to be negative, i.e.:

$$S_{IF} = \gamma_{MF\text{-}OF} - (\gamma_{IF\text{-}MF} + \gamma_{IF\text{-}OF}) < 0$$

or: $\boldsymbol{\gamma_{IF\text{-}OF} > \gamma_{MF\text{-}OF} - \gamma_{IF\text{-}MF}}$

Full dewetting is achieved when the spreading coefficient S_{OF} of the OF is positive, i.e.:

$$S_{OF} = \gamma_{IF\text{-}MF} - (\gamma_{MF\text{-}OF} + \gamma_{IF\text{-}OF}) > 0$$

or: $\boldsymbol{\gamma_{IF\text{-}OF} < \gamma_{IF\text{-}MF} - \gamma_{MF\text{-}OF}}$

Interfacial tension measurements for $\gamma_{IF\text{-}MF}$ and $\gamma_{MF\text{-}OF}$ were performed by KRÜSS GmbH using a spinning drop tensiometer and ADVANCE 1.11 software at room temperature and 2000–15500 rpm. IF was composed of 50 mM sucrose in distilled water, MF of 10 mg ml^{-1} soy PC in oleic acid and OF of 1wt% F108 + 200 mM sucrose in distilled water. The interfacial tension was computed from the resulting drop shape either with the Young-Laplace method or the Vonnegut method.

$\gamma_{IF\text{-}MF}$ was 11.05 ± 0.04 mN m^{-1} and $\gamma_{MF\text{-}OF}$ was 0.04 ± 0.01 mN m^{-1}. Considering that only partial dewetting took place at the current conditions and not full dewetting, we conclude that

1) $\boldsymbol{\gamma_{IF\text{-}OF} < \gamma_{IF\text{-}MF} + \gamma_{MF\text{-}OF} = 11.09\ mN\ m^{-1}}$
2) $\boldsymbol{\gamma_{IF\text{-}OF} > \gamma_{IF\text{-}MF} - \gamma_{MF\text{-}OF} = 11.01\ mN\ m^{-1}}$

That is, $\gamma_{IF\text{-}OF}$ should lie in the range between 11.01 mN m^{-1} and 11.09 mN m $^{-1}$.

1.7 Relation between surface area and volume reduction

To compute the volume of a sphere with radius *r* (deflated, fully dewetted vesicle) with a surface *a*, which corresponds to half of the area of the surface *A* of a sphere with radius *R* (assumption of a 50% dewetted vesicle with radius *R* before shrinking), we first compute *r*:

$a = 0.5*A$
$4\pi r^2 = 0.5*4\pi R^2$ and thus $r = R\sqrt{(0.5)}$

We then compute the new volume V_{new} of the dewetted vesicle using the value for *r*:

$V_{new} = 4/3\pi*r^3 = 4/3\pi*(R\sqrt{(0.5)})^3$

The relation between the reduced volume V_{new} and the initial volume V_{old} is therefore:

$V_{new}/V_{old} = [4/3\pi*(R\sqrt{(0.5)})^3] / [4/3\pi*R^3] = 0.5*\sqrt{(0.5)} = 0.35$

Assuming that a vesicle has half of its surface dewetted, the volume would need to be reduced to approx. one third (i.e. factor of 2*√2) so that its new surface matches the original dewetted bilayer area. The volume reduction was achieved by proportional osmotic ratio.

1.8 Microscopy

The observation of the processes inside the microfluidic chips and the fluorescent and bright-field images was done with a ZEISS Axio Observer 5 Microscope with a HXP 120 V light source and images were recorded with a ZEISS Axiocam 506 color microscope camera. Phantom V611 high-speed camera was used for the observation of the double emulsion production. The confocal images were recorded with a Leica TCS SPE confocal microscope.

1.9 Electroformation

Electroformation vesicles were prepared as follows: Soy PC was dissolved in methanol to a final concentration of 1 mg ml^{-1} and 20 µl aliquots were placed on two ITO coated glass slides (Sigma Aldrich) and dried under nitrogen for 20 min. A chamber was formed using a rubber spacer and the two slides and filled with 200 mM sucrose solution with additional 1 mM fluorescein dextran when testing encapsulation. The GUVs were formed by applying 1 V and 10 Hz for 4 h and 1.5 V and 4 Hz for 30 min. The GUVs were harvested by careful pipetting, stored at room temperature and used within 48 h after production.

Supporting Figures and Videos

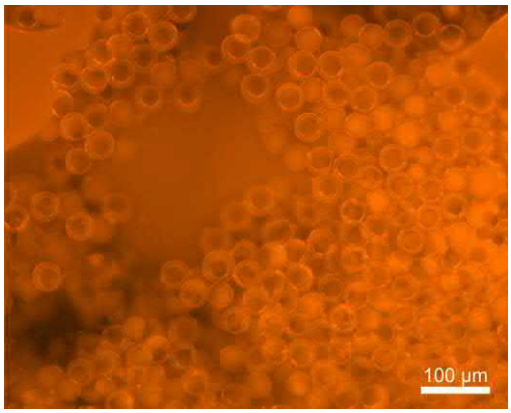

Figure S1: Fluorescent image of double emulsions after attempt for oil extraction with ethanol (24 h incubation, 28% ethanol in the outer fluid) as described in the literature [1]. Oleic Acid was stained with Nile Red.

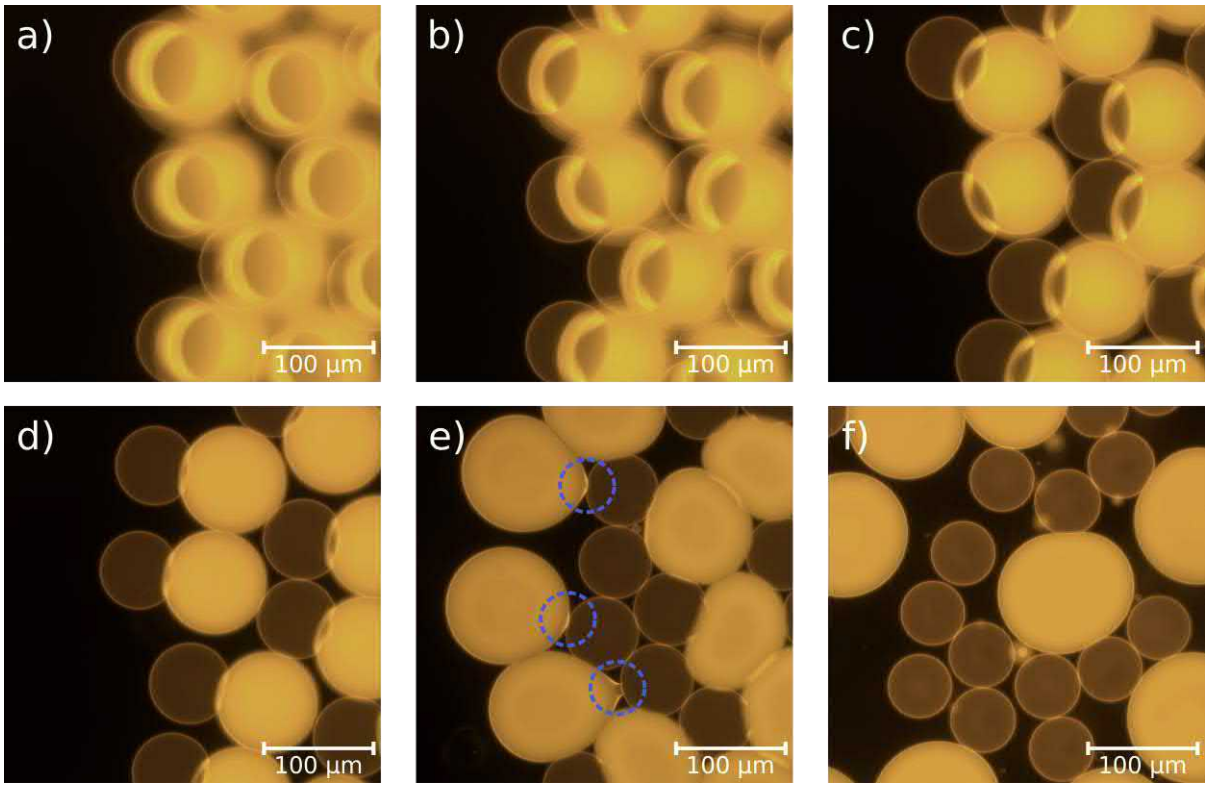

Figure S2: Dewetting process on a glass slide from a) to f). Shrinking of the vesicle turns partial dewetting (a-e) into full dewetting (f). The detachment step is clearly visible in (e) (blue circles). The time period of the whole process depends on the sample volume. In this case, the process from a) to f) took approx. 5 min. Fluorescent lipids (Liss-Rho-PE) were added to the MF for visualization of the vesicles (smaller and circular with thin membranes). Excess fluorescent lipids also stained the oil pockets (large, bright droplets).

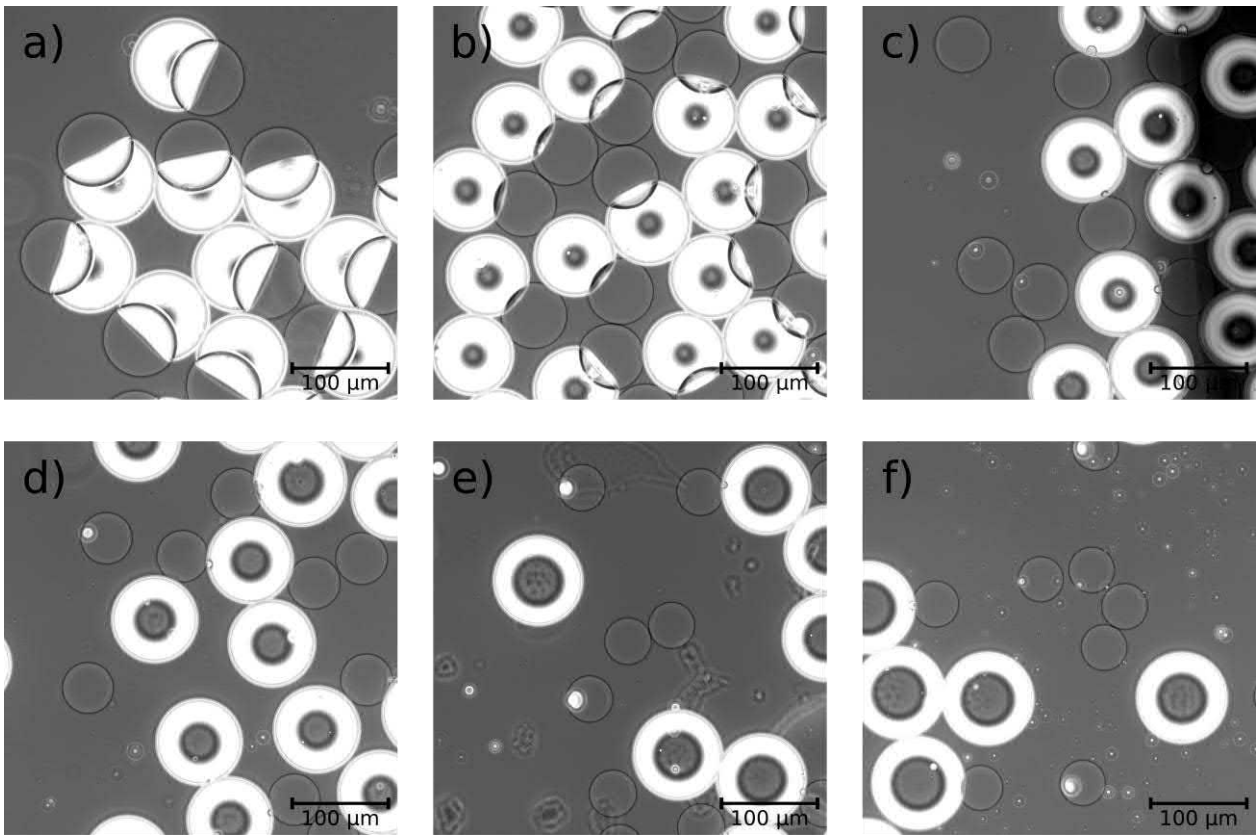

Figure S3: Phase contrast images of different sucrose concentration ratios between IF and OF showing the effect of vesicle deflation. a) 1:1 ratio (IF 25 mM, OF 25 mM) b) 1:2 ratio (IF 25 mM, OF 50 mM) c) 1:3 ratio (IF 25 mM, OF 75 mM) d) 1:4 ratio (IF 25 mM, OF 100 mM) e) 1:5 ratio (IF 25 mM, OF 125 mM) f) 1:6 ratio (IF 25 mM, OF 150 mM). A ratio of 1:3 or more results in full dewetting. Note that oil is bright, while vesicles are small circles with a thin dark membrane. The dark circles inside the bright oil droplets in figures (b-f) are an optical effect and not IF.

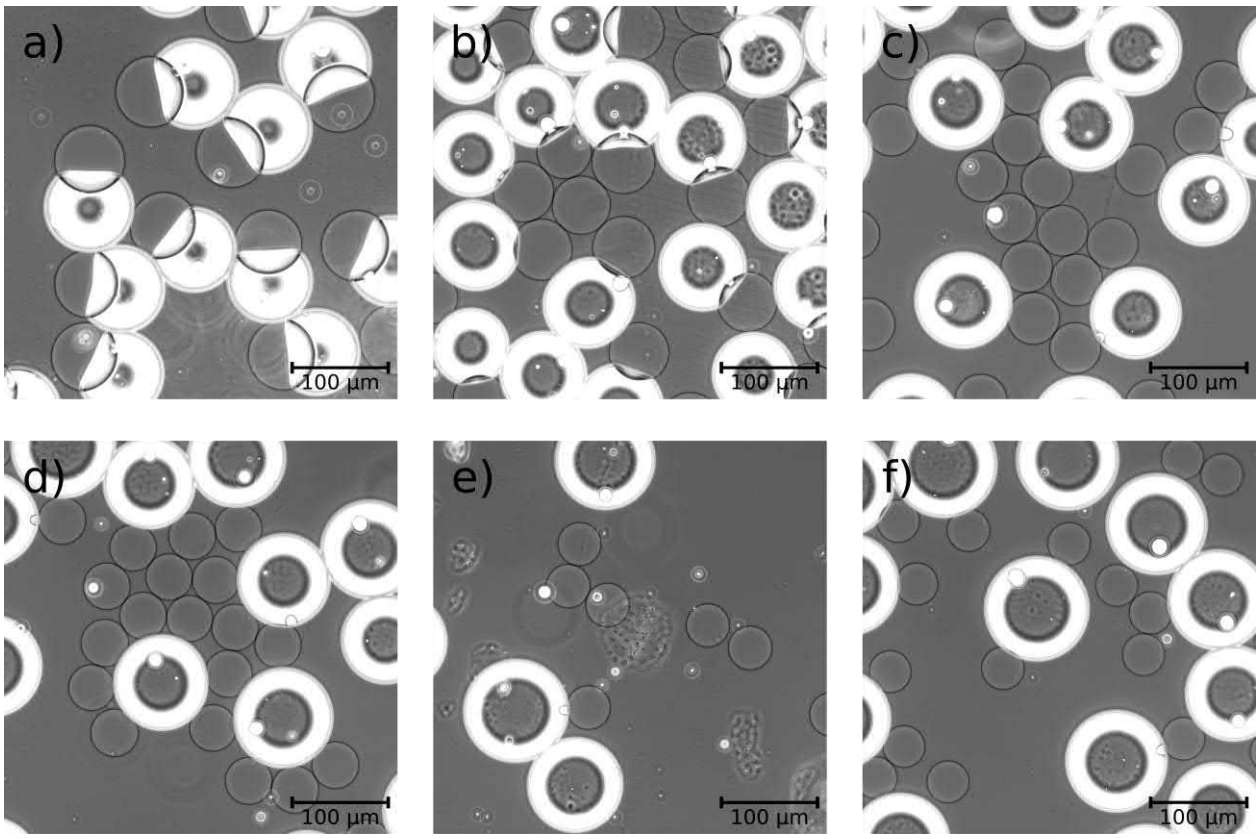

Figure S4: Different sodium chloride concentrations in IF and OF show that full dewetting due to vesicle deflation is independent of the osmolyte nature and can also be achieved with ionic molecules. a) 1:1 ratio (IF 25 mM, OF 25 mM) b) 1:2 ratio (IF 25 mM, OF 50 mM) c) 1:3 ratio (IF 25 mM, OF 75 mM) d) 1:4 ratio (IF 25 mM, OF 100 mM) e) 1:5 ratio (IF 25 mM, OF 125 mM) f) 1:6 ratio (IF 25 mM, OF 150 mM). Note that oil is bright, while vesicles are small circles with a thin dark membrane. The dark circles inside the bright oil droplets in figures (a-f) are an optical effect and not IF.

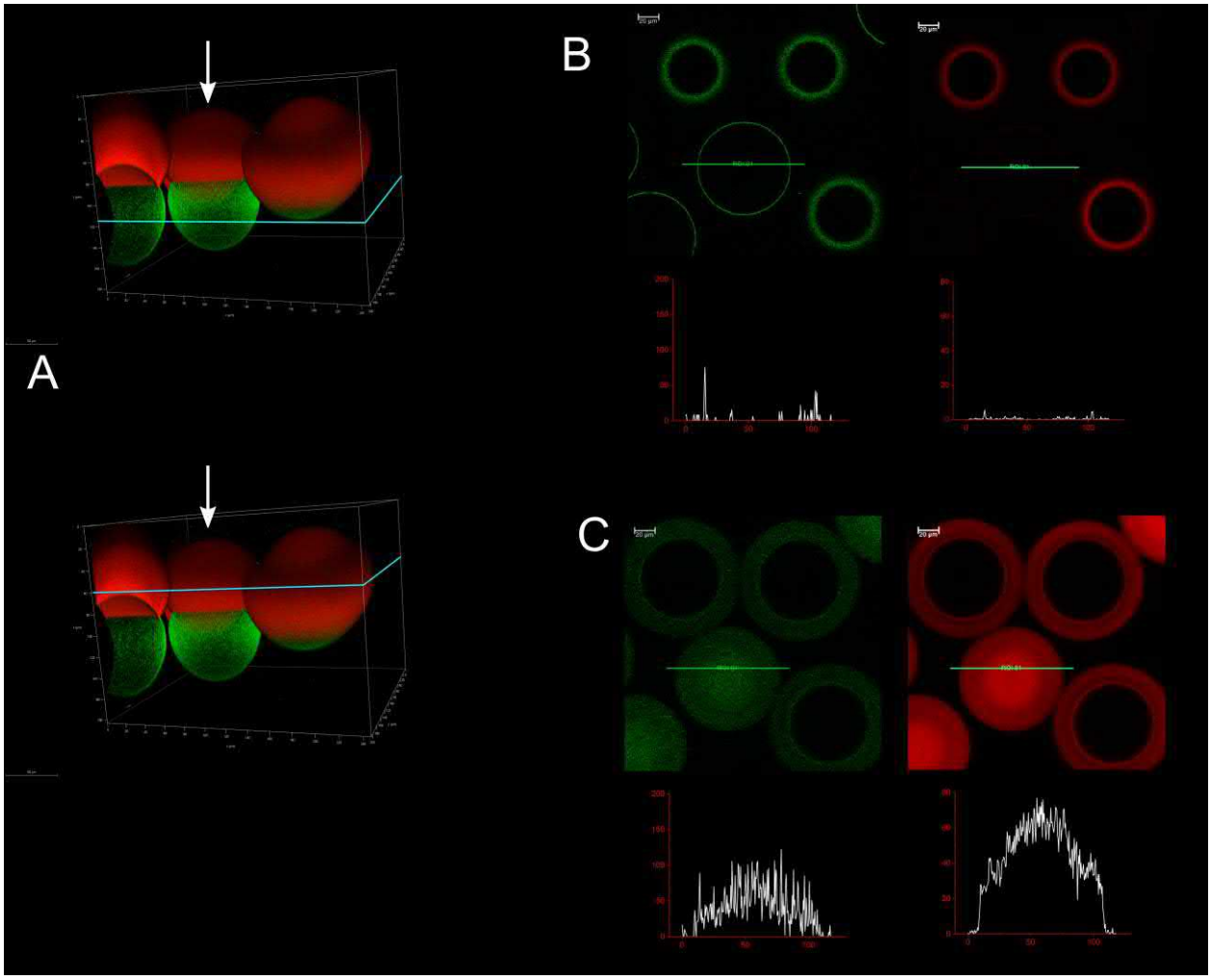

Figure S5: A. Z-stack from confocal images of partially dewetted (white arrow) and not dewetted vesicles. Oleic acid was stained with Nile red (red), while membranes were visualized through addition of fluorescent PE-CF lipids (green). **B.** Horizontal cross section of the lower, dewetted region of a vesicle (white arrow in **A**). The green stained membrane is clearly visible, while Nile red fluorescence is barely detectable. Diagrams show fluorescence intensity across the vesicle (green horizontal line) in arbitrary units. **C.** The oil pocket of the same vesicle is cross-sectioned showing both high green and red fluorescence intensity.

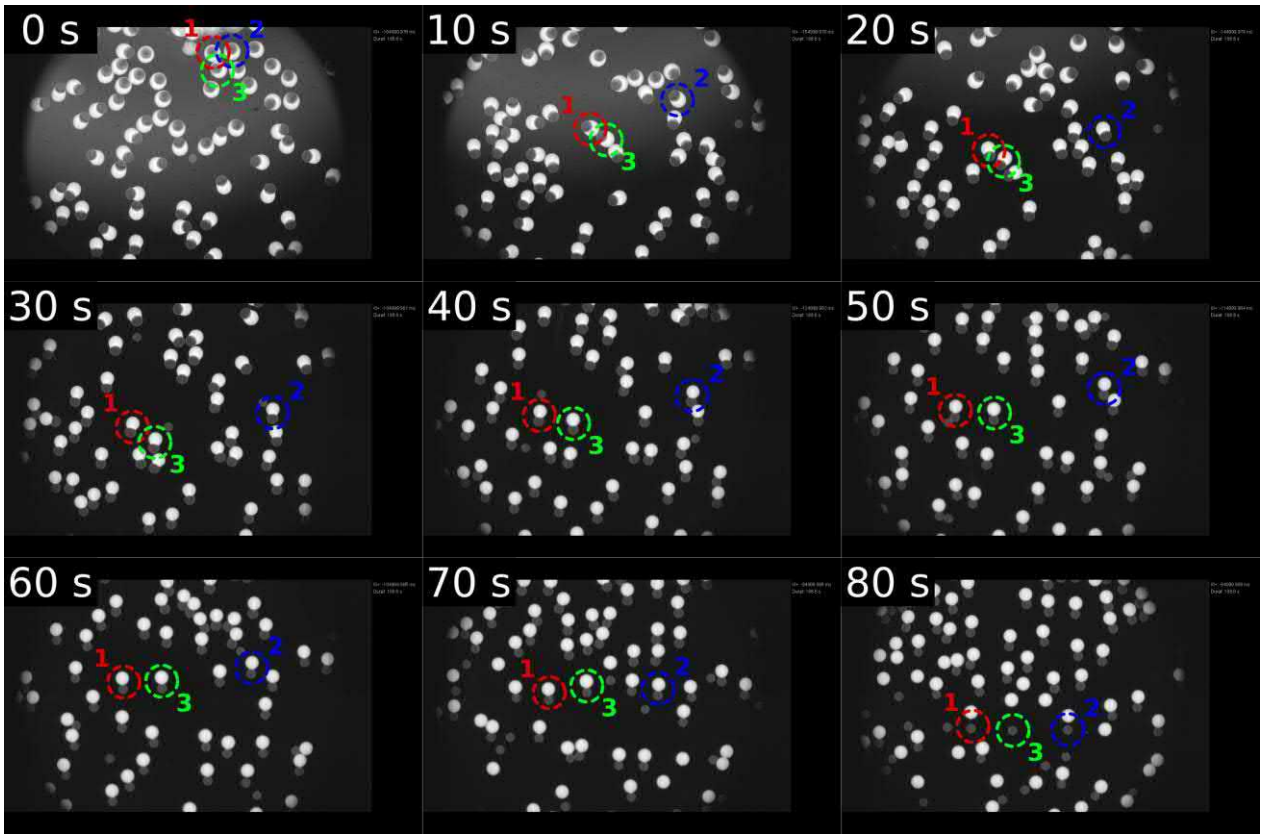

Figure S6: Snapshots from **Movie S2** showing the time scale of the dewetting process. Three individual double emulsions are highlighted (1-red, 2-blue, 3-green) and followed as they move along the chip length and undergo partial dewetting, shrinking and eventually detaching. Time stamps are given for each snapshot relative to the dewetting start of the selected vesicles (0 s = entering chip, no dewetting).

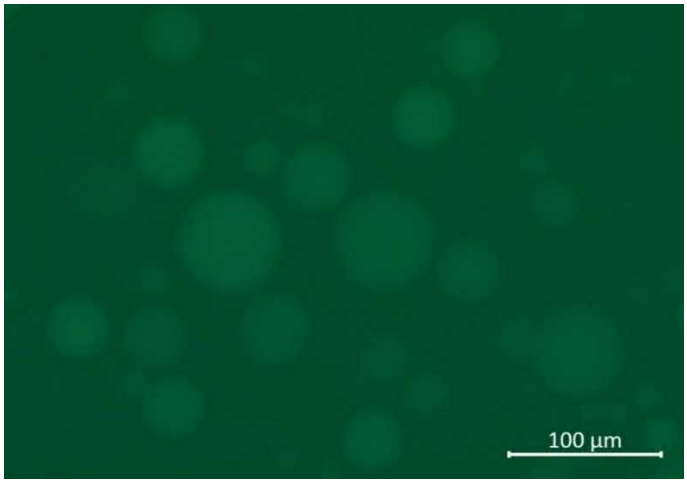

Figure S7: Fluorescent image of vesicles produced via electroformation in the presence of fluorescein isothiocyanate-dextran. Note that the water-soluble dye is present inside and outside of the vesicles. Prior to visualization, vesicles require washing.

Movie S1: Double emulsion production (bright field), showing w/o emulsion crossing the second junction. Original frame rate: 21 000 fps, video frame rate: 50 fps (420x slower)

Movie S2: Dewetting and oil pocket separation in microfluidic chip (Liss-Rho-PE fluorescence). Note that the camera is not static but follows the vesicles along the chip. Original frame rate: 24 fps, video frame rate: 125 fps (5x faster)

1. Petit, J., et al., *Vesicles-on-a-chip: A universal microfluidic platform for the assembly of liposomes and polymersomes.* The European Physical Journal E, 2016. **39**(6): p. 59.
2. Xia, Y. and G.M. Whitesides, *Soft lithography.* Angewandte Chemie International Edition, 1998. **37**(5): p. 550-575.
3. Whitesides, G.M., et al., *Soft lithography in biology and biochemistry.* Annual review of biomedical engineering, 2001. **3**(1): p. 335-373.
4. Deng, N. N., Yelleswarapu, M., & Huck, W. T., *Monodisperse Uni- and Multicompartment Liposomes.* Journal of the American Chemical Society **2016** 138 (24), 7584-7591, DOI: 10.1021/jacs.6b02107